

## Supplementary information for:

### Layered mixed tin-lead hybrid perovskite solar cells with high stability

Daniel Ramirez,<sup>a</sup> Kelly Schutt,<sup>b</sup> Zhiping Wang,<sup>b</sup> Andrew J. Pearson,<sup>c</sup> Edoardo Ruggeri,<sup>c</sup> Henry J. Snaith,<sup>b</sup> Samuel D. Stranks,<sup>c</sup> and Franklin Jaramillo<sup>a\*</sup>

a. Centro de Investigación, Innovación y Desarrollo de Materiales – CIDEMAT, Facultad de Ingeniería, Universidad de Antioquia UdeA, Calle 70 No. 52-21, Medellín, Colombia.

b. Department of Physics, University of Oxford, Clarendon Laboratory, Parks Road, Oxford, OX13PU, United Kingdom.

c. Cavendish Laboratory, Department of Physics, University of Cambridge, JJ Thomson Avenue, Cambridge CB3 0HE, UK

To optimize the FA/Cs ratio as basic structure for latter investigations on the dimensionality induced by the organic cation we prepared films with Cs as partial replacement of FA to form  $(t\text{-BA})_2(\text{FA}_{(1-x)}\text{Cs}_x)_2(\text{Pb}_{0.6}\text{Sn}_{0.4})_3\text{I}_{10}$  films ranging from  $x=0.05$  to  $x=0.20$ . As shown in Figure S1a-c, when more cesium was incorporated, the grain size increased to around 600 nm for  $x=0.15$ , while preserving the same film morphology. This was reflected in an improved absorption, steady state PL and TRPL lifetime. In contrast, the evident cracks in  $x=0.20$  had a negative impact in both, steady state PL and TRPL lifetime. The latter suggests that adding 15%Cs has a beneficial effect for both, improving film morphology and reducing non-radiative recombination.

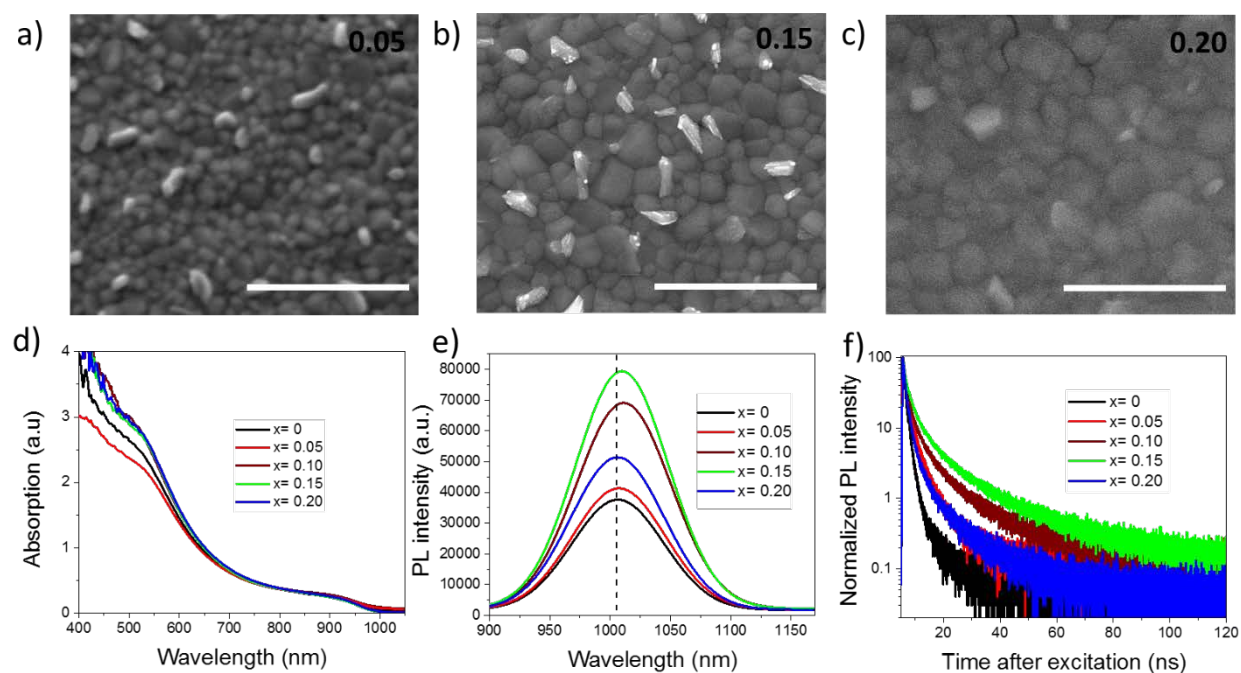


**Figure S1:**  $(t\text{-BA})_2(\text{FA}_{(1-x)}\text{Cs}_x)_2(\text{Pb}_{0.6}\text{Sn}_{0.4})_3\text{I}_{10}$  thin films. SEM images for a)  $x=0.05$ , b)  $x=0.15$  and c)  $x=0.20$ . Scale bar corresponds to  $2\mu\text{m}$ . d) Absorption, e) steady state PL and f) TRPL for  $x=0, 0.05, 0.10, 0.15$  and  $0.20$ .

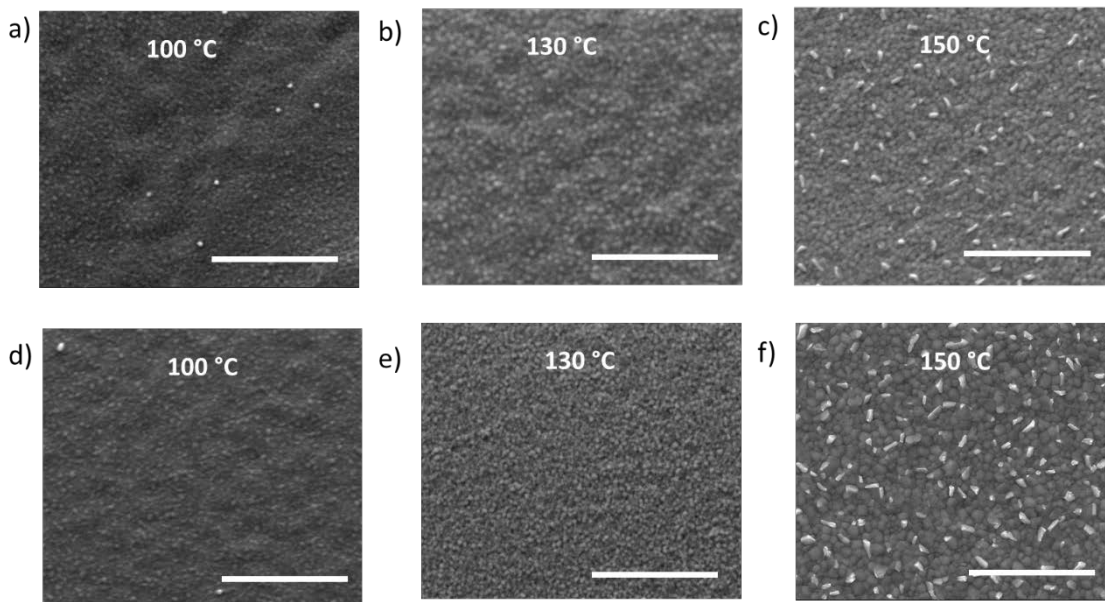


**Figure S2.** Comparative morphology of a-c)  $(t\text{-BA})_2(\text{FA})_2(\text{Pb}_{0.6}\text{Sn}_{0.4})_3\text{I}_{10}$  and d-f)  $(t\text{-BA})_2(\text{FA}_{0.95}\text{CS}_{0.05})_2(\text{Pb}_{0.6}\text{Sn}_{0.4})_3\text{I}_{10}$  thin films annealed at different temperatures. Scale bar corresponds to  $2\mu\text{m}$ .

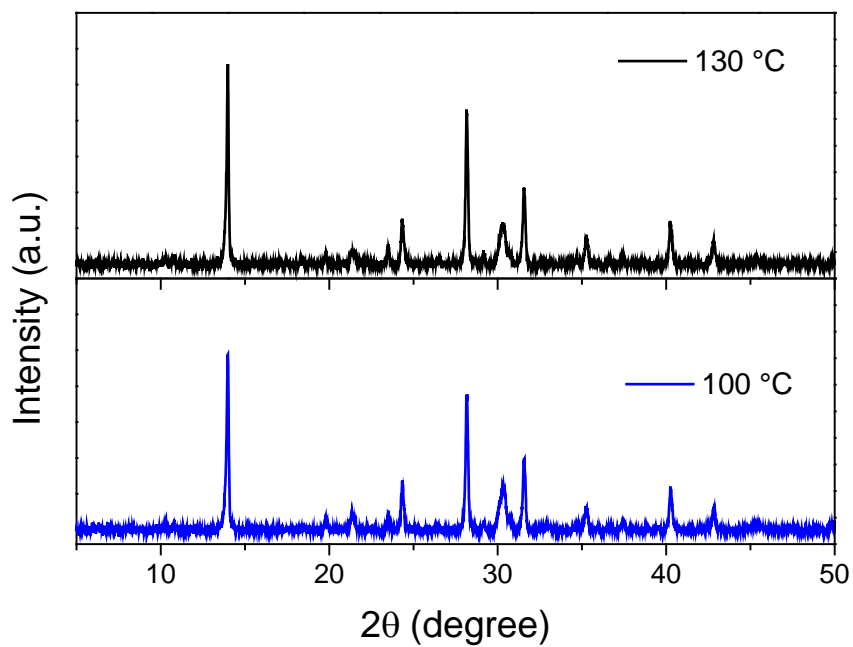


**Figure S3.** Comparative XRD pattern for  $(t\text{-BA})_2(\text{FA}_{0.95}\text{CS}_{0.05})_2(\text{Pb}_{0.6}\text{Sn}_{0.4})_3\text{I}_{10}$  thin films annealed at  $100\text{ }^\circ\text{C}$  and  $130\text{ }^\circ\text{C}$ .

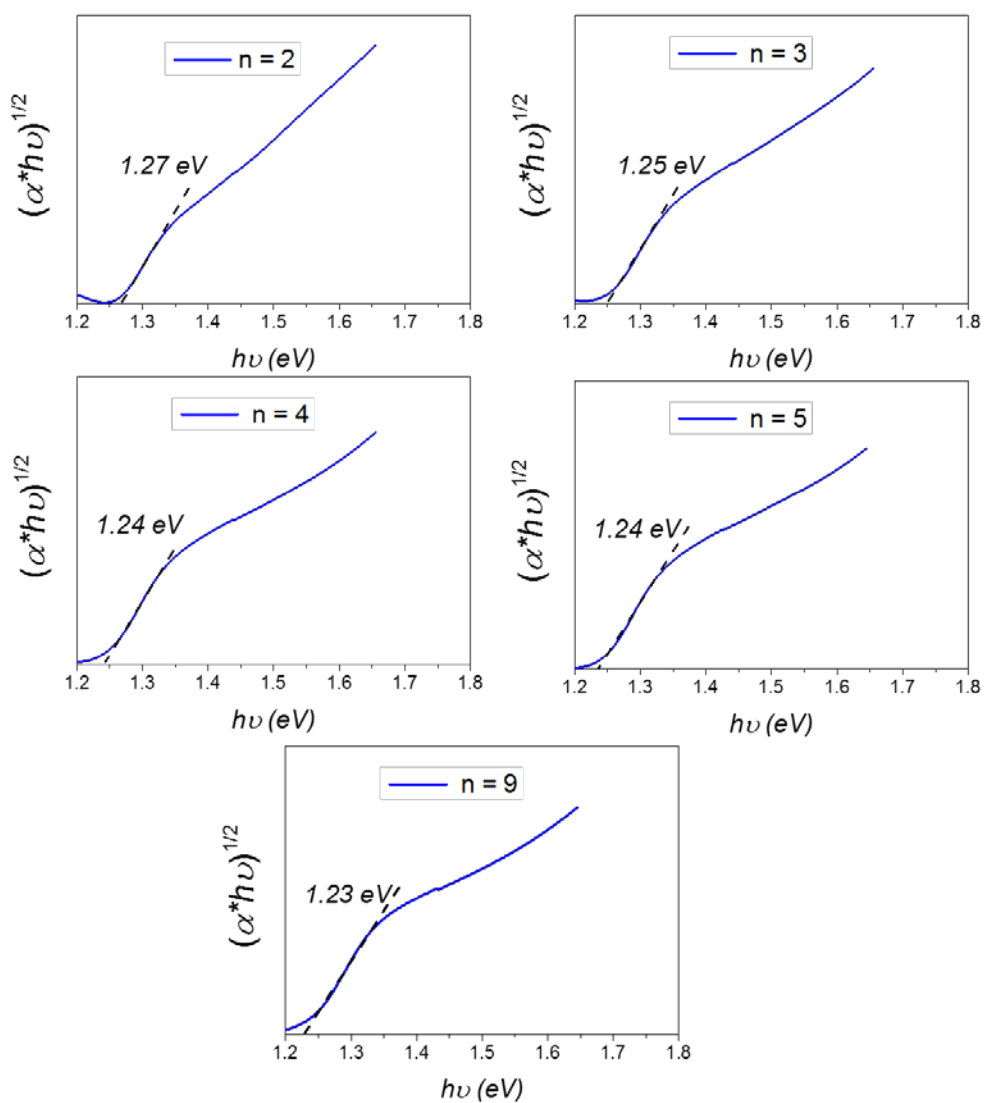


**Figure S4.** Tauc plots of  $(\text{t-BA})_2(\text{FA}_{0.85}\text{Cs}_{0.15})_{n-1}(\text{Pb}_{0.6}\text{Sn}_{0.4})_n\text{I}_{3n+1}$  thin films

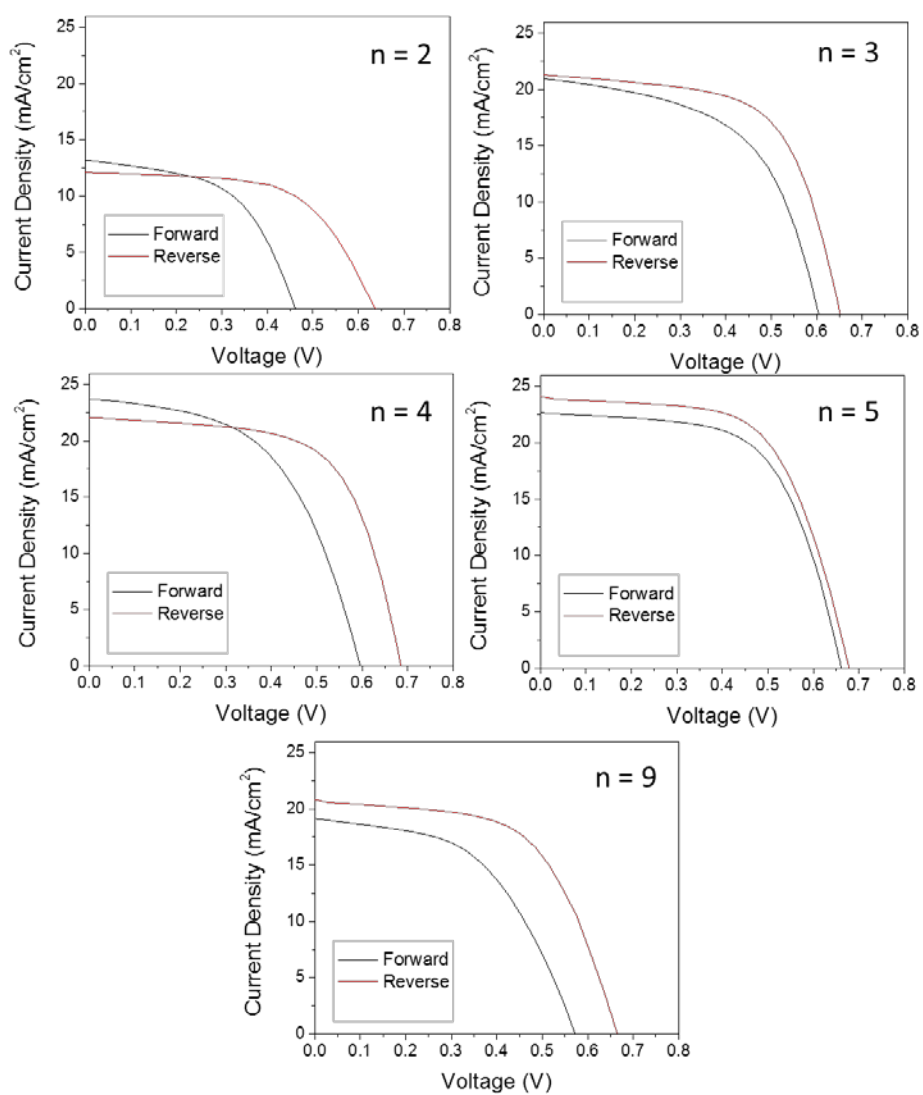


**Figure S5.** Forward and reverse scans for hybrid perovskite solar cells using  $(t\text{-BA})_2(\text{FA}_{0.85}\text{CS}_{0.15})_{n-1}(\text{Pb}_{0.6}\text{Sn}_{0.4})_n\text{I}_{3n+1}$  as active layer. a)  $J_{sc}$ , b)  $V_{oc}$  and c) FF.

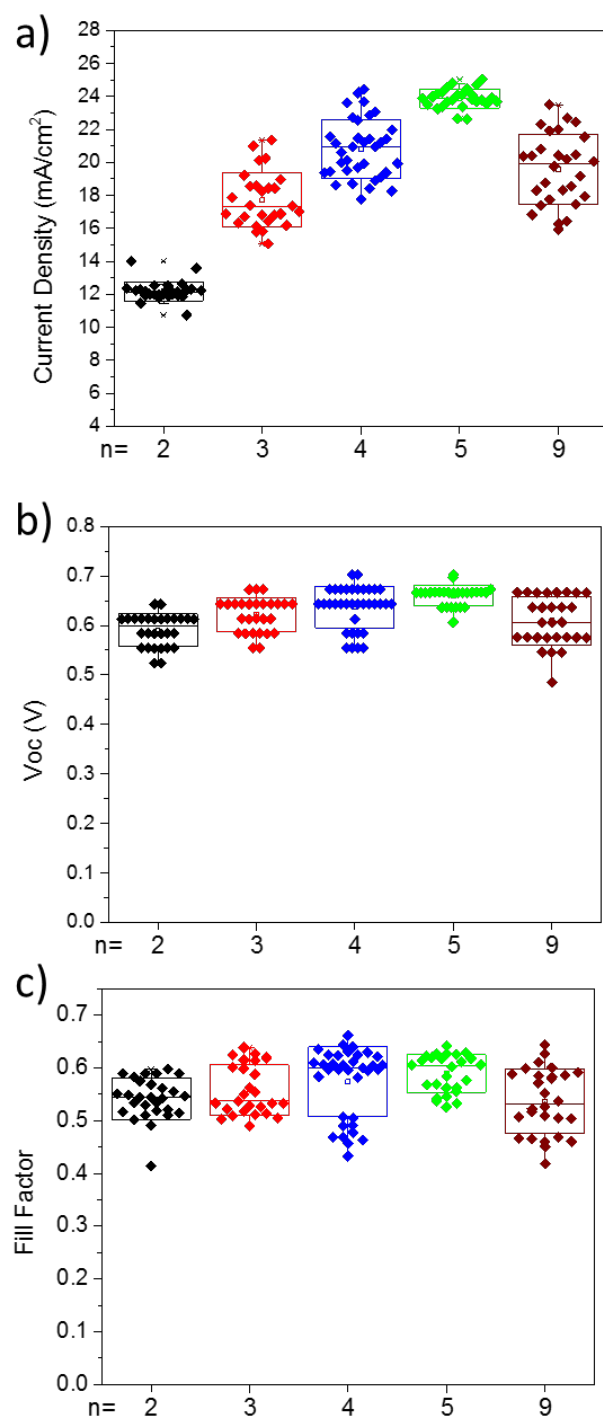


**Figure S6.** Complementary photovoltaic data for hybrid perovskite solar cells using  $(\text{t-BA})_2(\text{FA}_{0.85}\text{Cs}_{0.15})_{n-1}(\text{Pb}_{0.6}\text{Sn}_{0.4})_{n-1}\text{I}_{3n+1}$  as active layer. a)  $J_{sc}$ , b)  $V_{oc}$  and c) FF.

In Figure S6a, we show current density voltage (J-V) characteristics for all the cesium dependent samples. Average PCE in Figure S6b went from 3.2% for  $x=0$  up to 6.3% for both,  $x=0.10$  and  $x=0.15$  with the highest efficiency of 8.5% in the latter case, result of a short-circuit current ( $J_{sc}$ ) of 21.3  $\text{mA}/\text{cm}^2$ , fill factor (FF) of 0.60, and open-circuit voltage ( $V_{oc}$ ) of 0.64V. The previous findings for  $x=0.20$  suggested a low quality of the film, which led to a lower average PCE of 3.9%, limited by the low photocurrent. Other photovoltaic parameters are summarized in Table S1.

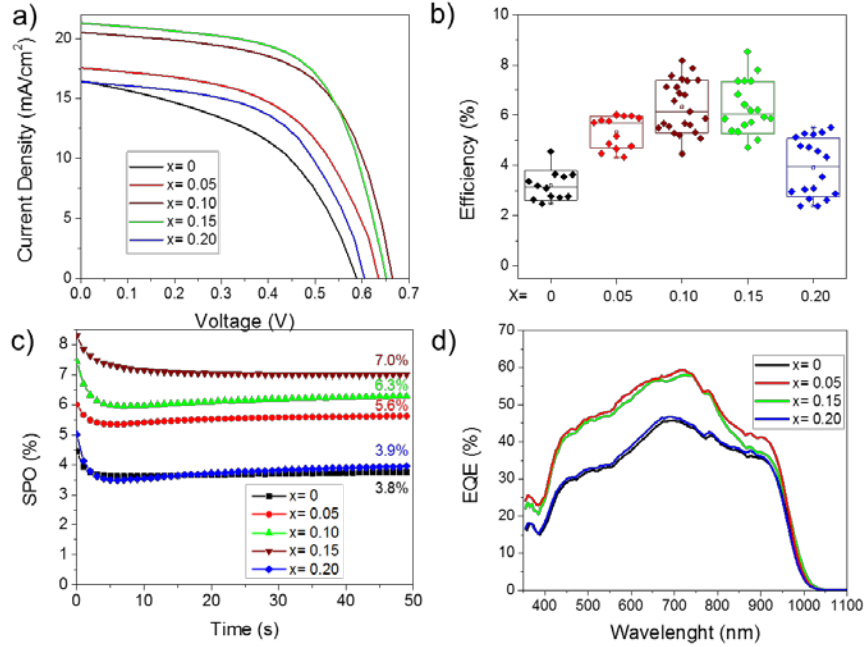


**Figure S7.** Photovoltaic performance of cesium dependent solar cells using  $(\text{t-BA})_2(\text{FA}_{(1-x)}\text{Cs}_x)_2(\text{Pb}_{0.6}\text{Sn}_{0.4})_3\text{I}_{10}$  as active layer. a) J-V curves, b) power conversion efficiency box plot, c) SPO and d) EQE.

**Table S1.** Cesium dependent solar cell performance parameters determined from J-V curves

Device	PCE (%)	Jsc ( $\text{mA}/\text{cm}^2$ )	$V_{oc}$ (V)	FF
<b><math>(\text{t-BA})_2(\text{FA})_2(\text{Pb}_{0.6}\text{Sn}_{0.4})_3\text{I}_{10}</math> (<math>x = 0</math>)</b>				
<i>Average</i>	$3.2 \pm 0.6$	$15.2 \pm 1.0$	$0.50 \pm 0.05$	$0.41 \pm 0.03$
<i>Champion</i>	3.6	15.1	0.55	0.43
<b><math>(\text{t-BA})_2(\text{FA}_{0.95}\text{Cs}_{0.05})_2(\text{Pb}_{0.6}\text{Sn}_{0.4})_3\text{I}_{10}</math> (<math>x = 0.05</math>)</b>				
<i>Average</i>	$5.3 \pm 0.6$	$17.6 \pm 0.5$	$0.58 \pm 0.06$	$0.52 \pm 0.04$
<i>Champion</i>	5.9	17.2	0.55	0.49
<b><math>(\text{t-BA})_2(\text{FA}_{0.90}\text{Cs}_{0.10})_2(\text{Pb}_{0.6}\text{Sn}_{0.4})_3\text{I}_{10}</math> (<math>x = 0.10</math>)</b>				
<i>Average</i>	$6.3 \pm 1.0$	$19.7 \pm 0.8$	$0.59 \pm 0.07$	$0.54 \pm 0.04$
<i>Champion</i>	7.8	19.9	0.67	0.59
<b><math>(\text{t-BA})_2(\text{FA}_{0.85}\text{Cs}_{0.15})_2(\text{Pb}_{0.6}\text{Sn}_{0.4})_3\text{I}_{10}</math> (<math>x = 0.15</math>)</b>				
<i>Average</i>	$6.3 \pm 1.0$	$18.3 \pm 1.6$	$0.62 \pm 0.03$	$0.55 \pm 0.04$
<i>Champion</i>	8.5	21.3	0.64	0.60
<b><math>(\text{t-BA})_2(\text{FA}_{0.80}\text{Cs}_{0.20})_2(\text{Pb}_{0.6}\text{Sn}_{0.4})_3\text{I}_{10}</math> (<math>x = 0.20</math>)</b>				
<i>Average</i>	$3.9 \pm 1.2$	$16.8 \pm 0.4$	$0.49 \pm 0.10$	$0.47 \pm 0.06$
<i>Champion</i>	5.5	16.4	0.61	0.42

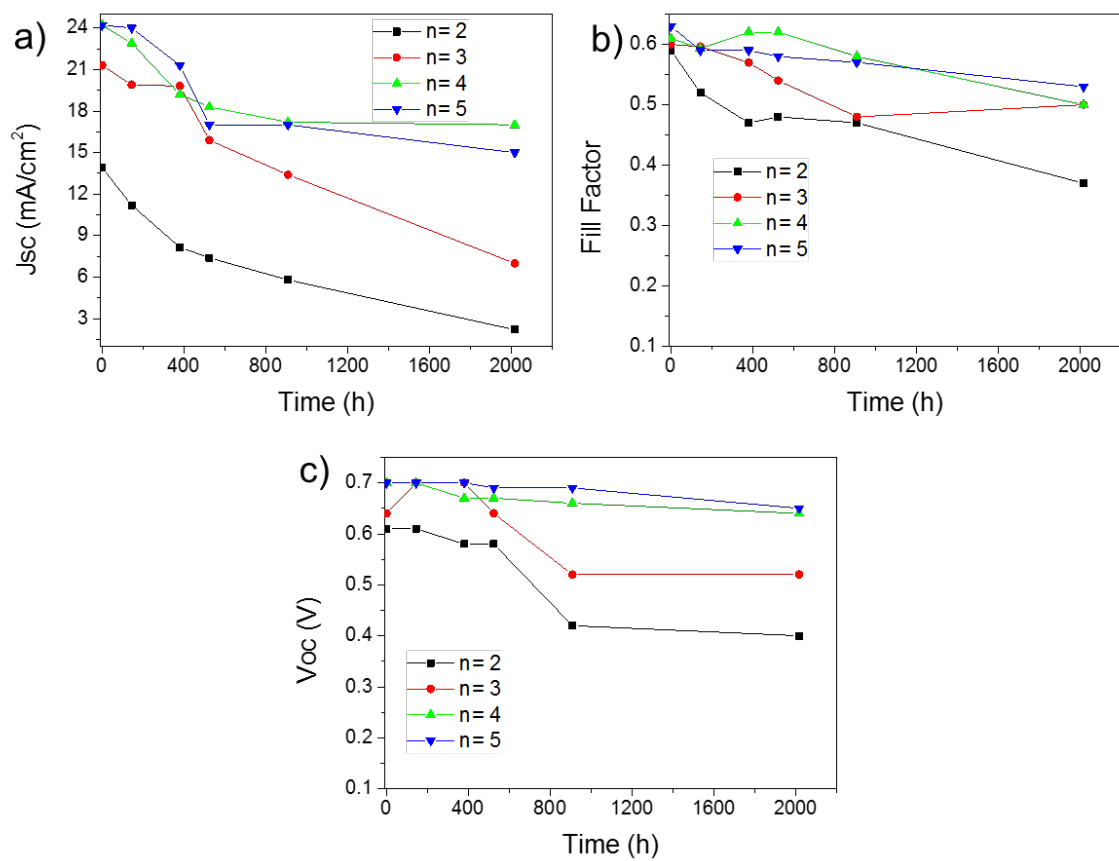


**Figure S8.** Evolution of the photovoltaic parameters over time for unencapsulated devices stored under nitrogen atmosphere.

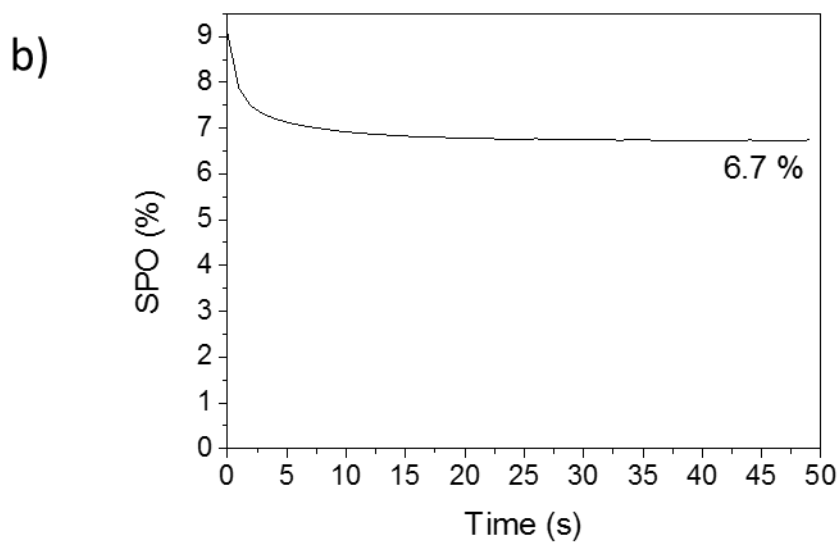
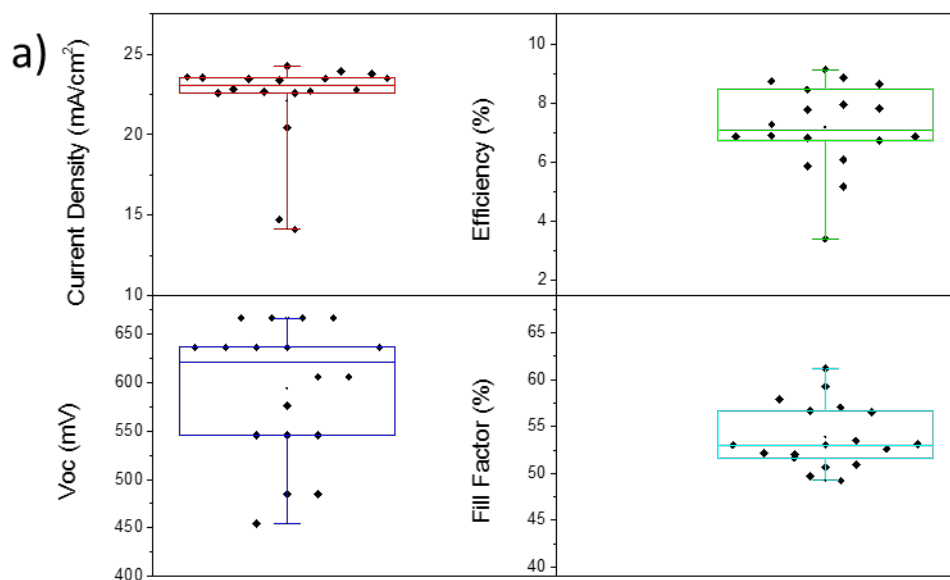


**Figure S9.** a) Photovoltaic parameters and b) SPO of hybrid perovskite solar cells with 3D (FA<sub>0.85</sub>CS<sub>0.15</sub>)(Pb<sub>0.6</sub>Sn<sub>0.4</sub>)I<sub>3</sub> as active layer.